Progress In Electromagnetics Research B, Vol. 25, 93–111, 2010

DATA-ADAPTIVE RESOLUTION METHOD FOR THE PARAMETRIC THREE-DIMENSIONAL INVERSION OF TRIAXIAL BOREHOLE ELECTROMAGNETIC MEASUREMENTS

F. O. Alpak † **and C. Torres-Verdín**

Department of Petroleum and Geosystems Engineering
University of Texas at Austin
1 University Station C0300, Austin, TX 78712-0228, USA

Abstract—We develop a new adaptive inversion procedure: Data-adaptive Resolution Inversion (DRI) method, which eliminates the need of selecting a parameterization prior to inversion. Instead, one performs a hierarchical search for the correct parameterization while solving a sequence of inverse problems with an increasing dimension of parameterization. A parsimonious approach to inverse problems usually involves the application of the same refinement consistently over the complete spatial domain. Such an approach may lead to over-parameterization, subsequently, to unrealistic conductivity estimates and excessive computational work. With DRI, the new parameterization at an arbitrary stage of inversion sequence is allocated such that new degrees of freedom are not necessarily introduced all over the spatial domain of the problem. The aim is to allocate new degrees of freedom only where it is warranted by the available data. Inversion results confirm that DRI is robust and efficient for multiparameter inversion of multicomponent borehole electromagnetic measurements.

1. INTRODUCTION

Accurate and reliable determination of hydrocarbon saturation is of principal importance for decisions regarding the exploration, development, and production of thinly-laminated sand-shale sequences typically encountered in deepwater turbidite reservoirs [28]. Thinly

Received 5 June 2010, Accepted 18 August 2010, Scheduled 25 August 2010
Corresponding author: F. O. Alpak (oalpak@yahoo.com).
† Now with Shell International Exploration and Production Inc., USA.

laminated sand-shale sequences are characterized by macroscopic electrical anisotropy, which in turn, could be interpreted as a good indicator of hydrocarbon pay [11]. In the case of horizontally layered formations with conductivity anisotropy, the value of conductivity parallel to the bedding plane differs from the one that is perpendicular to the bedding plane. Media of the above-described conductivity characteristics are also referred to as transversely anisotropic (TI or uniaxially anisotropic) conductive media. Often, high conductivity shale laminae dominate horizontal conductivity information on magnetic field measurements while information about vertical conductivity is predominantly determined by the low conductivity hydrocarbon-bearing sand laminae. In vertical boreholes penetrating horizontal layers, vertical dipole antennas of conventional induction logging tools detect signals from eddy currents that flow parallel to bedding plane. As such, they lack sensitivity to vertical conductivity, thereby causing underestimation of hydrocarbon reserves. This problem was identified as early as in 1930's by [17] and emphasized by [14]. Conversely, in highly-deviated and horizontal boreholes, conventional induction logging tools are more sensitive to the commonly encountered lower vertical conductivity. This behavior introduces difficulties in identifying marker beds for well-to-well correlation and for well geosteering.

Modern multicomponent induction logging tools were introduced by Baker-Hughes [12] and Schlumberger [16] to address the problems of conventional induction logging measurements in anisotropic rock formations. Baker-Hughes' tool measures five magnetic field components: H_{xx}, H_{yy}, H_{zz}, H_{xy}, and H_{xz}. On the other hand, Schlumberger's tool acquires measurements of all nine components of the magnetic field allowing closed-form determination of the azimuthal angle via a rotation of the tensor field measurements without resorting to inversion [22].

With the exception of [1], development of inversion algorithms for triaxial induction logging measurements has been focused to predominantly one- or, to a lesser extent, two-dimensional models [3, 5, 13, 15, 20, 22, 25–28].

A central problem when attempting to infer spatial distributions of conductivity from electromagnetic measurements is to explicitly honor the intrinsic spatial resolution of the measurements, i.e., the *a-priori* spatial parameterization of conductivity. Too low spatial resolution will result in measurements not being reconciled, while too high spatial resolution leads to unnecessary computational effort due to over-parameterization. In turn, over-parameterization, when not accurately regularized, often leads to increased non-uniqueness in the

inversion and ultimately causes spatial distributions of conductivity to be inconsistent with the physics of the measurements. The objective of this paper is to develop a data-adaptive resolution inversion method for the problem of multicomponent induction logging. We seek to circumvent the difficulty of estimating conductivity distributions with the correct spatial resolution by gradually increasing the resolution only at spatial locations warranted by the measurements. Thus, instead of proposing a fixed rigid resolution and subsequently seeking to invert the corresponding parameter set all at once with all the data available, we propose to solve a sequence of inversion problems with monotonically increasing resolution. DRI is related with the multigrid inversion method [4] in that it starts from the simplest (coarsest in the multigrid terminology) model and advances towards the most detailed (finest in the multigrid terminology) one. DRI algorithm by construction avoids the use of an artificial regularization parameter. From this viewpoint, DRI is philosophically akin to the trust-region method of [8], where the regularized solution is found by posing the regularization as a trust-region subproblem. DRI, on the other hand, embeds the regularization process to the adaptive refinement of the model parameterization based on the information content of the measurement data. Inversion approaches similar to DRI have been explored for the automatic history matching of fluid production measurements in the reservoir engineering literature [9]. Inspired by these ideas, we formulate a new data adaptive algorithm particularly suitable for inversion problems arising in borehole geophysics.

2. DATA-ADAPTIVE RESOLUTION INVERSION (DRI) METHOD

2.1. Overview

Conventional pixel-by-pixel inversion techniques attempt to compensate resolution discrepancies in the spatial domain due to overparameterization by penalizing deviations from *a-priori* knowledge about the sought solution. Bayesian estimation or Tikhonov regularization techniques [18, 19], for example, require the use of regularization parameters for this purpose. In many cases, the determination of regularization parameters is based on highly subjective grounds. DRI, on the other hand, can be viewed as a sequence of inversions where the parameterization for each level of estimation is a zonation. The resolution of the zonation is increased for each step in the sequence, i.e., progressive parameterization. This process is initiated by estimating a single parameter, namely, the average conductivity for the entire medium, using an arbitrary initial value. Then, the medium is

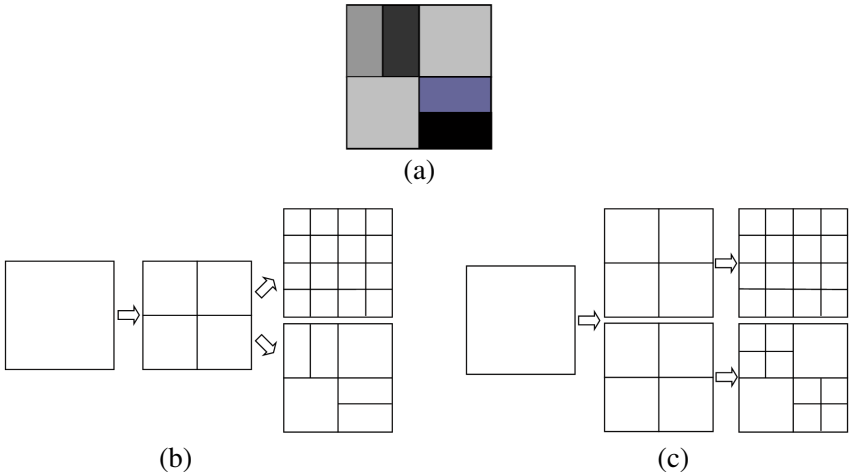

Figure 1. (a) A simple two-dimensional inverse problem. (b) Over-parameterization due to regular hierarchical refinement strategy versus ideal parameterization for the inverse problem-of-interest. (c) Regular hierarchical refinement strategy versus adaptive hierarchical refinement strategy.

split into 2^n equal-size subregions, where n is the spatial dimension of the conductive medium. A parameter is estimated for each subregion with initial values equal to the estimated parameter value for the entire conductive medium. In an approach that operates with first-order complexity following the first-step spatial splitting, each of these subregions can be divided into 2^n equal-size new subregions, and the refinement proceeds recursively with the powers of 2 until the convergence criteria are met to satisfaction. Let us denote the number of complexity levels by m. Then, the number of parameters to be a estimated in an arbitrary instance of inversion is given by $K = 2^{n\,(m-1)}$. It is self-evident that, K will increase rapidly as the sequential refinement process advances, especially for problems formulated in two- or three-dimensional spatial domains. In order to control the growth ratio for the number of parameters from one complexity level to the next while maintaining conformance to measurements, only a few new parameters are introduced at each level of the DRI.

2.2. Paradigm of DRI Algorithm on a Spatial Example

Figure 1 illustrates the DRI philosophy on a simple demonstrative two-dimensional spatial inverse problem adapted from [9]. Ideal

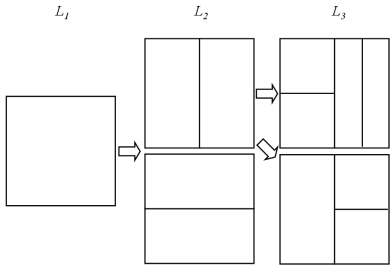

Figure 2. Example levels of refinement for the adaptive hierarchical refinement strategy (adapted from [9]). Three levels are shown in this figure. At the second level, vertical refinement is selected over horizontal refinement.

parameterization of the model for inversion is unknown while regular hierarchical refinement becomes too costly very rapidly. An adaptive hierarchical refinement strategy (Figure 2), as described by [9], can be devised that requires refinement indicators to guide the refinement process. At the second level, vertical refinement is selected over horizontal refinement.

Refinement criteria are developed to identify the focus region at each DRI level. New degrees of freedom are introduced only within the confines of this region. The principal philosophy of DRI relies on the goal of identifying the focus-region of (spatial and/or non-spatial) inversion model parameters and adapting its resolution to the spatial sensitivity of the measurements at each iteration level while avoiding unnecessary refinements.

DRI refinements are solely guided by objective criteria that stem from the information content of the measurements, specifically by the spatial sensitivity of the available measurements. In consequence, DRI eliminates subjective decisions that are artifacts of the rigid over-parameterization strategy of conventional pixel-by-pixel or parametric simultaneous inversion techniques. Decisions about the choice and magnitude of regularization parameters constitute an important example. By construction, DRI eliminates the need for artificial regularization parameters by adjusting the model resolution on the spatial domain based on the information warranted by the measurements.

2.3. DRI Algorithm for the Parametric Inversion of Borehole Geophysical Data

The spatial DRI algorithm described above (for simplicity) is reformulated to address the parametric inverse problems of borehole geophysics. For such problems, the inversion process starts with a simple parametric model. The initial model is constructed using a set of model parameters with the largest dominance on the reduction of the objective function. Identification of this set of model parameters is achieved at the first assessment level, also called the first complexity assessment-advancement level. Once the level of model complexity is determined, the inversion phase starts (complexity level inversion phase). Nonlinear inversion iterations are advanced until the improvement in the inverted model becomes insignificant or the reduction of the objective function indicates that complexity level convergence is attained. This, in turn, triggers the next complexity assessment-advancement level of the adaptive inversion. Assessment-advancement level involves the identification of the most relevant set of new model parameters and their introduction to the inversion process. Subsequent to each assessment-advancement level, DRI reverts back to the inversion phase. The data-adaptive inversion process advances through a number of complexity assessment-advancement and complexity level inversion phases until the complexity assessment-advancement phase determines that the next advancement will be statistically insignificant. Since the model complexity is continuously adjusted to the information content of the measurements, by construction the DRI algorithm avoids the use of artificial regularization parameters. Consequently, DRI eliminates the uncertainty introduced by the subjective choice of artificial regularization. This is by no means a claim that the uncertainty in the inverted model is completely eliminated. In fact, uncertainty is still prevalent, yet, the uncertainty in the inverted model stems purely from imperfect observations (measurements) collected at finite locations and from finite angles within the unknown model. Elimination of subjective regularization parameters renders the DRI an adequate tool for uncertainty analysis. At the inversion phase, the DRI solver minimizes the objective function expressed by a pure data misfit given by

$$C(\mathbf{x}) = [\mathbf{m} - S(\mathbf{x})]^T \mathbf{C}_D^{-1} [\mathbf{m} - S(\mathbf{x})] \tag{1}$$

and subject to physical value-range constraints on the vector of model parameters, $\mathbf{x}$. In Equation (1), $\mathbf{m}$ denotes the vector of multicomponent electromagnetic measurements and $\mathbf{C}_D$ represents the covariance matrix of measurement errors. The vector of simulated

measurements is given by $S(\mathbf{x})$. In principle, any optimization method can be utilized to compute model parameters by minimizing the objective function of Equation (1) at each level of DRI complexity. Optimization techniques that require the gradient of the objective function are less intense in terms of computational effort per iteration. Techniques that require the computation of a sensitivity matrix are computationally more demanding compared to gradient-based optimization techniques but generally entail more rapid convergence. In practice, the optimal choice of optimizer is problem dependent. DRI's focus-region tracking logic makes use of the data sensitivity matrix to sort through various parameterizations and select the most suitable ones to proceed further. In this paper, we implement a sensitivity-matrix-based optimization method to naturally complement the DRI technique. The DRI optimization engine is implemented using a least-squares Gauss-Newton minimization algorithm embedded in a dual finite-difference grid stencil [21]. Mathematical details of the DRI complexity assessment-advancement phase are documented in the Appendix A.

3. FORWARD MODEL

Simulation of triaxial induction logging measurements is carried out using a three-dimensional anisotropic electromagnetic forward model. The forward model consists of solving Maxwell's equations in the frequency domain and assumes a time-harmonic variation of the form $e^{i\omega t}$, where t is time, $i = \sqrt{-1}$, $\omega = 2\pi f$ is angular frequency, and f is linear frequency (Hz). For arbitrary 3D, inhomogeneous, electrically anisotropic media and assuming SI units, Maxwell's equations in the presence of impressed electric current sources are given by

$$\nabla \times \mathbf{E} = -i\omega\mu_o\mathbf{H}, \tag{2}$$

$$\nabla \times \mathbf{H} = \bar{\bar{\sigma}}'\mathbf{E} + \mathbf{J}_p, \tag{3}$$

and

$$\nabla \cdot \mathbf{B} = 0, \tag{4}$$

where $\mathbf{E}$ and $\mathbf{H}$ are the electric- and magnetic-field vectors, respectively and $\mathbf{B}$ is the magnetic flux density vector. We assume that the medium under consideration does not exhibit spatial variations of magnetic permeability, whereupon the magnetic field and flux density are related by $\mathbf{B} = \mu_o\mathbf{H}$, where $\mu_o = 4\pi\times10^{-7}$ (H/m) is the magnetic permeability of free space. In Equation (3), $\mathbf{J}_p$ is the impressed electrical-source-current density vector, $\bar{\bar{\sigma}}' = \bar{\bar{\sigma}} + i\omega\,\varepsilon\bar{\bar{\mathbf{I}}}$ is the complex conductivity tensor, $\bar{\bar{\sigma}}$ is the ohmic conductivity tensor, ε is dielectric permittivity, and $\bar{\bar{\mathbf{I}}}$ is the unity dyad.

Electromagnetic field equations are solved on Yee's staggered grid [24] using a finite-difference algorithm described in [10]. In this implementation, electromagnetic equations are transformed into a second-order coupled scalar-vector potential formulation prior to finite-difference discretization. The resulting code accurately simulates borehole electromagnetic logging measurements acquired with multicomponent magnetic transmitters and receivers. An anisotropic conductivity-averaging scheme is implemented following the guidelines of [23]. Computational efficiency of the forward modeling algorithm is further enhanced using an optimal geometric finite-difference gridding technique [6].

4. NUMERICAL EXAMPLE

In a numerical example, we consider inversion of synthetic multicomponent electromagnetic measurements generated from a transversely anisotropic invaded (by the mud-filtrate) single-layer model (Figure 3). A hydrocarbon-saturated sand layer is assumed to be buried in an isotropic background (shale) with a conductivity of 0.1 S/m. In addition to mud-filtrate invasion, we consider the presence of a conductive annulus between the invaded and uninvaded zones. Conductivity values are chosen consistent with the physics of fresh

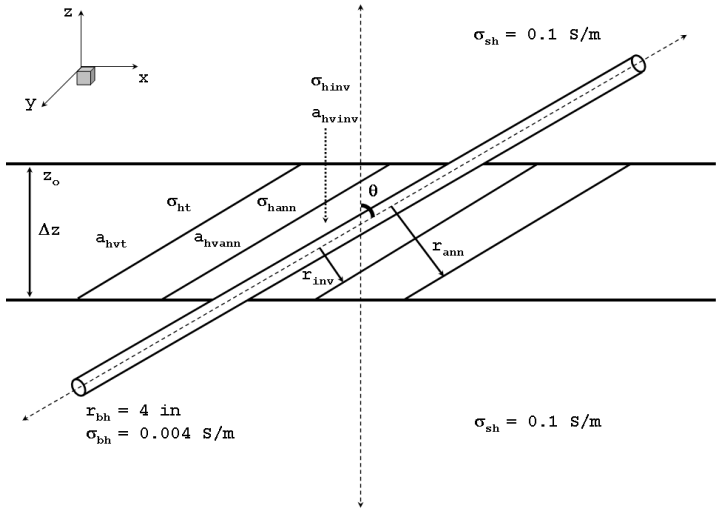

Figure 3. Example single-layer model for the parametric inversion of multicomponent induction logging measurements.

Table 1. Summary of inversion results for the single invaded layer example. Parameter values that are subject to inversion at a given DRI level are typed with boldface characters along with parameter values estimated by GNI.

MODEL PARAMETER	MODEL UNIT	INITIAL MODEL	DRI L1 MODEL	DRI L2 MODEL	DRI L3 MODEL	DRI L4 MODEL	DRI L5 MODEL	GNI MODEL	TRUE MODEL
Θ	[degree]	55.00	**59.36**	**59.39**	**59.95**	**59.69**	**60.03**	**56.40**	60.00
σ_{ht}	[S/m]	0.100	**0.011**	**0.014**	**0.015**	**0.012**	**0.013**	**0.019**	0.013
a_{hvt}	[dimensionless]	1.00	1.00	**1.95**	**2.16**	**2.47**	**2.48**	**1.83**	2.50
z_o	[ft]	-4.08	-4.08	-4.08	**-4.02**	**-4.05**	**-4.02**	**-3.96**	-4.00
Δz	[ft]	8.16	8.16	8.16	**8.00**	**8.06**	**8.00**	**8.04**	8.00
σ_{hinv}	[S/m]	0.100	0.100	0.100	0.100	**0.052**	**0.012**	**0.007**	0.010
a_{hvinv}	[dimensionless]	1.00	1.00	1.00	1.00	**1.56**	**1.48**	**1.02**	1.50
r_{inv}	[in]	15.00	15.00	15.00	15.00	**8.68**	**10.13**	**12.30**	10.00
σ_{hann}	[S/m]	0.100	0.100	0.100	0.100	0.100	**0.023**	**0.020**	0.025
a_{hvann}	[dimensionless]	1.00	1.00	1.00	1.00	1.00	**1.41**	**1.31**	1.50
r_{ann}	[in]	25.00	25.00	25.00	25.00	25.00	**19.50**	**21.60**	20.00
No of inverted parameters:		-	2	3	5	8	11	11	-
No of Gauss-Newton Iterations (since the last adaptation):		-	2	2	4	7	5	22	-
No of Gauss-Newton Iterations (total):		-	2	4	8	15	20	22	-

water-base mud-filtrate invasion into a formation saturated with high-salinity residual aqueous and movable hydrocarbon phases (see, for more details, [7]). The true model parameters are displayed in Table 1.

The model parameters subject to inversion are divided into five classes. Each class contains parameters that are relatively more closely associated with each other as warranted by the physics of the electromagnetic induction problem-of-interest. Relatively more traditional model parameters of induction logging inversion are distributed among the classes that appear earlier in the adaptive iterative inversion process. Whereas less common model parameters that characterize the detailed features of the near-borehole conductivity field are consolidated to classes that are introduced subsequently to the inversion process. Definitions of the model parameters subject to inversion (Table 1 and Figure 3) and their classification are as follows: *Class 1:* θ = dip angle of the borehole penetrating through the rock formation, σ_{ht} = horizontal conductivity of the uninvaded rock formation, and a_{hvt} = transverse anisotropy ratio of the uninvaded rock formation (= σ_{ht}/σ_{vt}, horizontal conductivity divided by the vertical conductivity of the uninvaded rock formation); *Class 2:* z_o = vertical location of the formation-top and Δz = thickness of the rock formation; *Class 3:* σ_{hinv} = horizontal conductivity of the mud-filtrate invaded zone, a_{hvinv} = transverse anisotropy ratio of the mud-filtrate invaded zone (= $\sigma_{hinv}/\sigma_{vinv}$, horizontal conductivity divided by the vertical conductivity of the mud-filtrate invaded zone),

and r_{inv} = radius of the mud-filtrate invaded zone; *Class 4:* σ_{hann} = horizontal conductivity of the annulus, a_{hvann} = transverse anisotropy ratio of the annulus (= $\sigma_{hann}/\sigma_{vann}$, horizontal conductivity divided

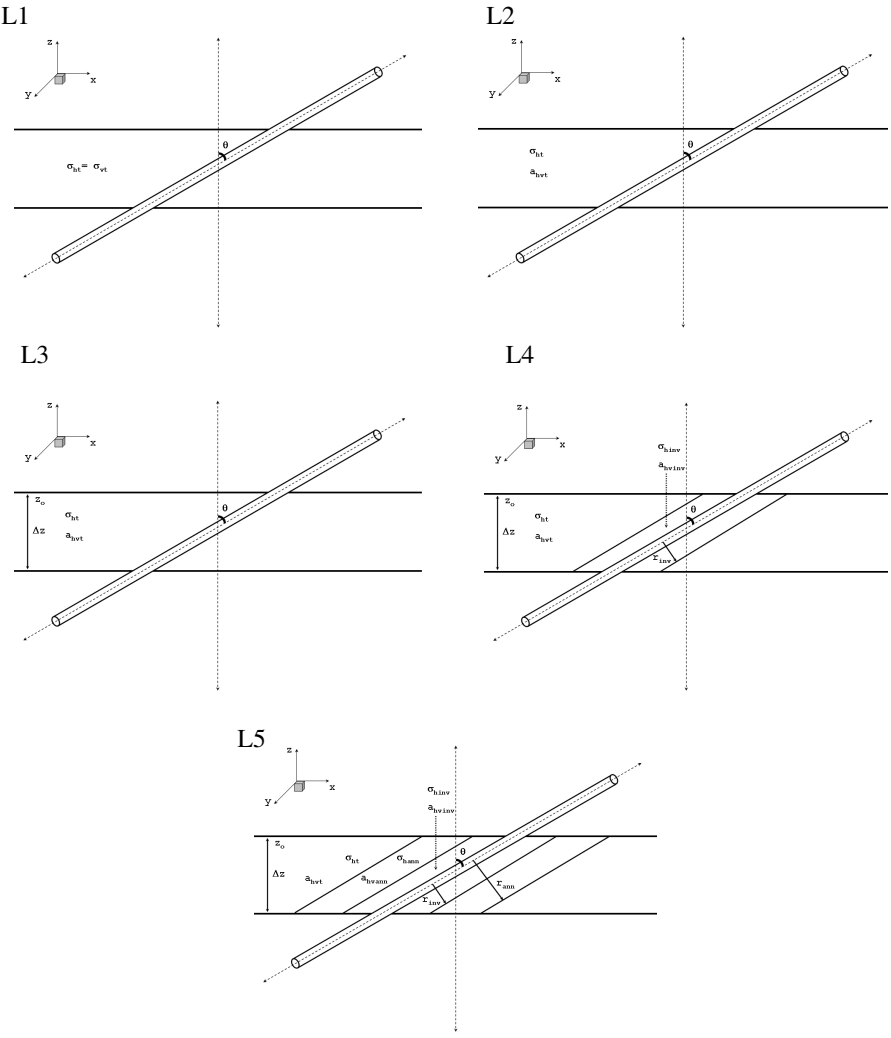

Figure 4. Five levels of the adaptive hierarchical parametric refinement strategy [L1 through L5]. Multicomponent induction logging inverse problem: single-layer example. Each figure panel associated with a given level of refinement displays the model parameters inverted at that particular level.

by the vertical conductivity of the annulus), and r_{ann} = radius of the annulus. In our implementation, if DRI identifies at least one of the model parameters within a given class to be of value for including in the inversion problem, the full-set of parameters (within that class) are added to the inversion problem. The only exception is *Class 1.* While σ_{ht} and θ are closely associated with each other (characterizing a simple, homogeneous and isotropic deviated-well problem), a_{hvt} is added separately to the inversion process (changing the nature of the simple isotropic problem to an anisotropic one). The forward model also employs known model parameters whose values remain unchanged over the course of the inversion (Figure 3): σ_{sh} = isotropic background (shale) conductivity, borehole conductivity, and r_{bh} = borehole radius.

Triaxial induction logging measurements are simulated for a single-frequency (20 kHz) single-transmitter induction logging tool with six multicomponent receivers. Measurements are acquired in an inclined borehole with a dip angle of 60°, and simulated for 40 logging stations across the −20 ft to +20 ft (true relative vertical depth) interval. In total, $40 \times 6 \times 5$ measurements are used for inversion. The measurements are contaminated with 0.1% Gaussian random noise. The above-described parametric variant of the DRI is applied to solve the inverse problem.

The relative progress of adaptive refinements performed by DRI is shown in the panels of Figure 4. Table 1 describes the level-by-level inversion results. Adaptive inversion process begins with the iterations that aim for reconstructing the model parameters σ_{ht} and θ. Remaining model parameters are set to their initial-guess values. DRI proposes the addition of a_{hvt} to the set of inverted model parameters subsequent to two Gauss-Newton iterations (rendering the complete set of *Class 1* parameters active for inversion). *Class 2*, *Class3*, and *Class 4* model parameters are stepwise added to the inversion process subsequent to two, four, and seven iterations after the most recent adaptation, respectively. The convergence criterion is satisfied after five iterations subsequent to the L4-to-L5 model transition. Table 1 also documents the inversion results obtained by applying a weighted and additive-regularized conventional Gauss-Newton inversion (GNI) technique such as the one described in [2]. The regularization parameter is selected as 1.0×10^{-2}. No experimentation was carried out to identify the optimal value for the regularization parameter. Both DRI and GNI methods are run until they satisfy a dimensionless misfit criterion. The iterations cease once the misfit reduces below the noise level, namely, 1.0×10^{-3}. Figure 5 shows the post-inversion (DRI) data fit. Synthetic measurements and post-inversion simulated electromagnetic data are displayed for an example receiver location.

DRI reveals a hierarchy of importance among model parameters by adaptively assimilating the information content of multicomponent electromagnetic induction measurements. Uninvaded formation conductivity and layer geometry characteristics dominate over invaded

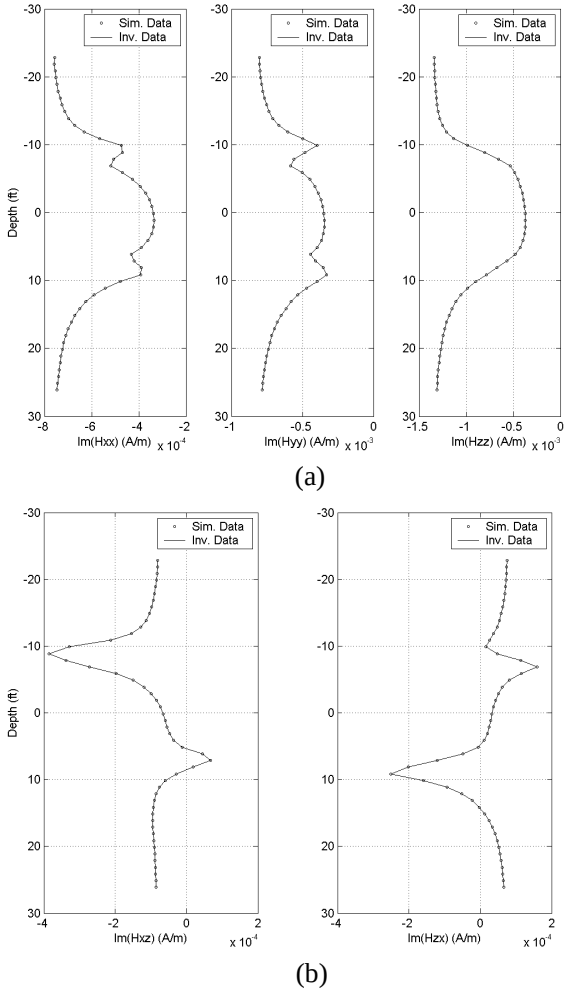

Figure 5. Post-inversion data fit for an example receiver location. Imaginary part of the measured and post-inversion magnetic field are shown for every relevant coupling direction. Note that, for the transversely anisotropic problem-of-interest, the following holds with regards to the magnetic field measurements: $H_{xy} = H_{yx} = H_{yz} = H_{zy} = 0$.

zone and annulus characteristics. DRI identifies a more accurate inversion result within a fewer number of Gauss-Newton iterations compared to GNI. Except for the final (L5) phase, all other phases of the DRI employ fewer than eleven parameters in contrast to the GNI. Thus, on average, the cost of computing the Gauss-Newton Hessian matrix is considerably cheaper for DRI over the course of inversion. Data misfit attained via DRI decreases rapidly between the phases L1 and L3. The phases L4 and L5 demand additional iterations to deliver further reductions in the data misfit. Our experience indicates that DRI is typically three to four times faster than GNI on a given inversion problem. It is important to emphasize the fact that tests carried out by feeding various initial models to DRI and GNI lead to similar results for the problem-of-interest. Therefore, our conclusions about the auspicious features of DRI hold independent of the initial model.

5. DISCUSSION

DRI technique completely eliminates the need for an artificial regularization parameter and the inevitable requirement of experimentation component that stems from it. In our experience, DRI technique performs particularly well for parametric inversion problems where a physically based classification of model parameters is possible, such as the one described above.

It is important to emphasize the fact that the adaptivity criterion of DRI assumes that the measurement errors abide by the random distribution. It is currently not known how DRI would perform on measurement data contaminated with correlated noise. At present, adaptivity is unidirectional within DRI. The algorithm sequentially refines the model parameterization. Further research on adaptive inversion techniques may lead to algorithms where both adaptive refinement and coarsening are possible. In terms of implementation, the DRI technique is notably more complex compared to conventional inversion techniques that rely on a single-scale parameterization.

Although DRI was tested with 20 kHz induction logging data in this work, it is worthwhile to comment about the impact of the use of different frequencies on DRI results. Assuming that the noise level of the measurement data remains unchanged, we expect that relatively deeper features, e.g., uninvaded formation conductivity values, could potentially be more accurately recovered with moderately lower frequency data. The first phases of DRI may also incur lower computational costs (fewer iterations) to yield the same level of accuracy that would be obtained if 20 kHz data were

employed. However, the reduced spatial resolution would almost certainly negatively influence the inversion of smaller scale near-borehole features such as invaded and annulus zone properties. It is possible that relatively more detailed refinement levels are not reached at all over the course of adaptations when considerably lower frequency data is used in DRI. On the other hand, use of notably higher frequency data would greatly increase the non-uniqueness of the inversion of conductivity features that are away from the borehole. Having stated that, smaller scale near-borehole features and bed-boundary locations could potentially be more accurately resolved with moderately higher frequency induction data. It is our opinion that DRI inversion of multi-frequency triaxial induction logging measurements can be very beneficial for the improved accuracy of inversion results and for the enhanced stability of the inversion process, especially, with increased levels of noise contaminating the measurement data.

6. CONCLUSION

We formulated and implemented a data-adaptive inversion technique for the estimation of spatial distributions of conductivity from borehole electromagnetic field measurements by operating on relatively coarse scales. For cases where the true conductivity distribution contains fine-scale variations, DRI is guided to introduce new degrees of freedom as spatially complex as warranted by the measurements, thereby eliminating subjective regularization decisions that introduce artificial biases to the inversion process. The algorithm relies on progressive spatial domain refinement in conjunction with sequential parameter estimation. Focus-region identification and tracking criteria are utilized to prevent over-parameterization. DRI algorithm by construction avoids the use of artificial regularization parameters. Inversion results validate the robustness and computational efficiency of DRI.

For the electromagnetic test problem evaluated in this paper, DRI shows that uninvaded formation conductivity and layer geometry parameters have a larger influence on the inversion outcome compared to model parameters that describe the invaded zone and the annulus. DRI yields a more accurate inversion result by entailing a fewer number of iterations in comparison to GNI. Overall, the unit computational cost of DRI is lower than GNI.

ACKNOWLEDGMENT

Funding for the work reported in this paper was provided by UT Austin's Research Consortium on Formation Evaluation, jointly sponsored by BP, Baker Hughes, ConocoPhillips, ENI E&P, ExxonMobil, Halliburton, Mexican Institute for Petroleum, OXY, Petrobras, Weatherford, Schlumberger, Shell, Statoil, and TOTAL.

APPENDIX A. DATA-ADAPTIVE PARAMETERIZATION

Introduction of new parameters will facilitate reduction of the objective function, but it will also increase computational cost and, in general, increase parameter uncertainty. Therefore, the parameterization must be selected in a proper way to obtain a reliable result.

In order to select the most productive parameterization, it would be helpful to know the minimum objective function values, $\min_{\mathbf{x}} C$, achievable with each potential parameterization refinement. This is, however, clearly unattainable because of the high computational costs associated with performing the corresponding minimizations numerically.

In order to circumvent such costly computations, the predicted attainable objective function value, $\tilde{C}$, is introduced. $\tilde{C}$ corresponds to $\min_{\mathbf{x}} C$ when $S(\mathbf{x})$ is linear. When using a least-squares formulation, such as Equation (1), linearization of $S(\mathbf{x})$ will make the objective function quadratic in $\mathbf{x}$. Conventional techniques for calculating the minimum of a quadratic function lead to the following analytic expression:

$$\tilde{C}(\boldsymbol{\tau}_Q) = \Delta\mathbf{m}_Q^T(\mathbf{C}_D^{-1} - \mathbf{D}_Q)\Delta\mathbf{m}_Q, \tag{A1}$$

$$\mathbf{D}_Q = \mathbf{C}_D^{-1}\mathbf{J}_Q(\mathbf{J}_Q^T\mathbf{C}_D^{-1}\mathbf{J}_Q)^{-1}\mathbf{J}_Q^T\mathbf{C}_D^{-1}, \tag{A2}$$

where $\boldsymbol{\tau}_Q$ denotes a parameterization containing Q parameters. $\mathbf{J}_Q$ denotes the sensitivity matrix for the parameterization $\boldsymbol{\tau}_Q$. $\Delta\mathbf{m}_Q = \mathbf{m} - S(\mathbf{x}_Q)$ denotes the current residual. Evaluation of $\tilde{C}$ involves calculation of the sensitivity matrix for the refined parameterization at a single point in the model space, as opposed to a full minimization for evaluating $\min_{\mathbf{x}} C$. In order to find the best parameterization $\boldsymbol{\tau}_Q$ with Q parameters, $\tilde{C}$ for different parameterizations containing Q parameters are compared. The parameterization with the lowest $\tilde{C}$ value is the best choice with Q parameters (local winner). Local winners for different numbers of parameters are then compared in order to find the parameterization to be used in the next step of the estimation sequence.

Generally, an increase in the number of the parameters will decrease the value of $\tilde{C}$. Hence, selecting the parameterization with the lowest $\tilde{C}$ will introduce as many new parameters as necessary. Therefore, it is not optimal to have only the smallest $\tilde{C}$ value as the selection criterion to determine the number of new parameters to be introduced. A measure of the uncertainty in $\tilde{C}$ is also needed to assess whether the reduction in $\tilde{C}$ due to the introduction of an increased number of parameters is significant.

The measurement errors are random, thus, $\tilde{C}$ is also random. The standard deviation, $\sigma(\tilde{C})$, can be used as a measure of the uncertainty in $\tilde{C}$. It can be shown that

$$\sigma\left\{\tilde{C}(\boldsymbol{\tau}_Q)\right\} = \left[4E\left\{\tilde{C}(\boldsymbol{\tau}_Q)\right\} - 2(M-Q)\right]^{1/2}, \tag{A3}$$

where E denotes statistical expectation and M is the number of (electromagnetic) measurements. $E(\tilde{C})$ will however depend on the difference between the true model parameters and the estimated model parameters (conductivity, layer thickness, etc.) at the current stage in the estimation sequence, and is therefore unknown. Following [9], we approximate $E(\tilde{C})$ by $\tilde{C}$, leading to

$$\sigma\left\{\tilde{C}(\boldsymbol{\tau}_Q)\right\} \cong \upsilon\left\{\tilde{C}(\boldsymbol{\tau}_Q)\right\} = \left[4\tilde{C}(\boldsymbol{\tau}_Q) - 2(M-Q)\right]^{1/2}. \tag{A4}$$

An increase in the number of inverted model parameters will reduce $\tilde{C}$. However, if $\tilde{C}(\boldsymbol{\tau}_{Q+1}) + \upsilon\{\tilde{C}(\boldsymbol{\tau}_Q)\} \geq \tilde{C}(\boldsymbol{\tau}_Q)$, the reduction is not considered to be significant. Consequently, $\boldsymbol{\tau}_Q$ is selected as the new parameterization.

The sequence of estimations is terminated when the value of the objective function can be explained by random measurement errors. This situation occurs when $C(\boldsymbol{\tau}_Q)$ is sufficiently close to the expected value of C at the solution of the inverse problem at hand, namely, $E(\hat{C})$. Then, the standard deviation $\sigma(\hat{C})$ emerges as a good measure of closeness. We choose "sufficiently close" to be one standard deviation. Then, the estimation sequence is terminated when the following inequality is satisfied

$$C(\boldsymbol{\tau}_Q) < E(\hat{C}) + \sigma(\hat{C}), \tag{A5}$$

which can be restated as

$$C(\boldsymbol{\tau}_Q) < (M-Q) + [2(M-Q)]^{1/2}. \tag{A6}$$

Termination will also be triggered whenever the criterion for the introduction of new parameters advises against introducing more parameters.

REFERENCES

1. Abubakar, A., T. M. Habashy, V. Druskin, S. Davydycheva, H. Wang, T. Barber, and L. Knizhnerman, "A three-dimensional parametric inversion of multi-component multi-spacing induction logging data," *Society of Exploration Geophysicists International Exposition and 74th Annual Meeting*, Denver, Colorado, 2004.
2. Alpak, F. O., T. M. Habashy, C. Torres-Verdín, and E. B. Dussan V., "Joint inversion of transient-pressure and time-lapse electromagnetic logging measurements," *Petrophysics*, Vol. 45, 251–267, 2004.
3. Anderson, B., T. Barber, and T. M. Habashy, "The interpretation and inversion of fully triaxial induction data," *Transactions of 43rd Annual Logging Symposium: Society of Professional Well Logging Analysts*, Paper O, Oiso, Japan, 2002.
4. Borcea, L., "Nonlinear multigrid for imaging electrical conductivity and permittivity at low frequency," *Inverse Problems*, Vol. 17, 329–359, 2001.
5. Cheryauka, A. B. and M. S. Zhdanov, "Focusing inversion of tensor induction logging data in anisotropic formations and deviated well," *Society of Exploration Geophysicists International Exposition and 71st Annual Meeting*, San Antonio, Texas, 2001.
6. Druskin, V. and L. Knizhnerman, "Gaussian spectral rules for three-point second differences: I. A two-point positive definite problem in a semi-indefinite domain," *SIAM J. Numer. Anal.*, Vol. 37, 403–422, 1999.
7. George, B. K., C. Torres-Verdín, M. Delshad, R. Sigal, F. Zouioueche, and B. Anderson, "Assessment of in-situ hydrocarbon saturation in the presence of deep invasion and highly saline connate water," *Petrophysics*, Vol. 45, 141–156, 2003.
8. Goharian, M., M. Soleimani, and G. Moran, "A trust region subproblem for 3D electrical impedance tomography inverse problem using experimental data," *Progress In Electromagnetics Research*, Vol. 94, 19–32, 2009.
9. Grimstad, A.-A., T. Mannseth, G. Nævdal, and H. Urkedal, "Adaptive multiscale permeability estimation," *Computational Geosciences*, Vol. 7, 1–25, 2003.
10. Hou, J., R. K. Mallan, and C. Torres-Verdín, "Finite-difference simulation of borehole EM measurements in 3D anisotropic media using coupled scalar-vector potentials," *Geophysics*, Vol. 71, G225–G233, 2006.
11. Klein, J. D., P. R. Martin, and D. F. Allen, "The petrophysics

of electrically anisotropic reservoirs," *Transactions of 36th Annual Logging Symposium: Society of Professional Well Logging Analysts*, Paper HH, Paris, France, 1995.

12. Kriegshäuser, B., O. Fanini, S. Forgang, G. Itskovich, M. Rabinovich, L. Tabarovsky, L. Yu, M. Epov, and J. van der Horst, "A new multicomponent induction logging tool to resolve anisotropic formations," *Transactions of 40th Annual Logging Symposium: Society of Professional Well Logging Analysts*, Paper D, Keystone, Colorado, 2000.
13. Kriegshäuser, B., S. McWilliams, O. Fanini, and L. Yu, "An efficient and accurate pseudo 2-D inversion scheme for multicomponent induction log data," *Society of Exploration Geophysicists International Exposition and 71st Annual Meeting*, San Antonio, Texas, 2001.
14. Kunz, K. S. and J. H. Moran, "Some effects of formation anisotropy on resistivity measurements in boreholes," *Geophysics*, Vol. 23, 770–794, 1958.
15. Lu, X. and D. Alumbaugh, "One-dimensional inversion of three-component induction logging in anisotropic media," *Society of Exploration Geophysicists International Exposition and 71st Annual Meeting*, San Antonio, Texas, 2001.
16. Rosthal, R., T. Barber, S. Bonner, K. Chen, S. Davydycheva, G. Hazen, D. Homan, C. Kibbe, G. Minerbo, R. Schlein, L. Villegas, H. Wang, and F. Zhou, "Field test results of an experimental fully-triaxial induction logging tool," *Society of Exploration Geophysicists International Exposition and 73rd Annual Meeting*, Dallas, Texas, 2003.
17. Schlumberger, C., M. Schlumberger, and E. G. Leonardon, "Some observations concerning electrical measurements in anisotropic media and their interpretation," *Transactions of the American Institute of Mining Engineers*, Vol. 100, 159–182, 1934.
18. Tarantola, A., *Inverse Problem Theory: Methods for Data Fitting and Model Parameter Estimation*, Elsevier, Amsterdam, 1987.
19. Tikhonov, A. N. and V. Y. Arsenin, *Solution of Ill-posed Problems*, John Wiley, New York, 1977.
20. Tompkins, M. J. and D. L. Alumbaugh, "A transversely anisotropic 1-D electromagnetic inversion scheme requiring minimal a priori information," *Society of Exploration Geophysicists International Exposition and 72nd Annual Meeting*, Salt Lake City, Utah, 2002.
21. Torres-Verdín, C., V. L. Druskin, S. Fang, L. A. Knizhnerman, and A. Malinverno, "A dual-grid nonlinear inversion technique

with applications to the interpretation of dc resistivity data," *Geophysics*, Vol. 65, 1733–1745, 2000.

22. Wang, H., T. Barber, R. Rosthal, J. Tabanou, B. Anderson, and T. Habashy, "Fast and rigorous inversion of triaxial induction logging data to determine formation resistivity anisotropy, bed boundary position, relative dip, and azimuth angles," *Society of Exploration Geophysicists International Exposition and 73rd Annual Meeting*, Dallas, Texas, 2003.
23. Wang, T. and S. Fang, "3-D electromagnetic anisotropy modeling using finite differences," *Geophysics*, Vol. 66, 1386–1398, 2001.
24. Yee, K. S., "Numerical solution of initial boundary value problems involving Maxwell's equations in isotropic media," *IEEE Transactions on Antennas and Propagation*, Vol. 14, 302–307, 1966.
25. Yu, L., B. Kriegshäuser, O. Fanini, and J. Xiao, "A fast inversion method for multicomponent induction log data," *Society of Exploration Geophysicists International Exposition and 71st Annual Meeting*, San Antonio, Texas, 2001.
26. Zhang, Z., L. Yu, B. Kriegshäuser, and R. Chunduru, "Simultaneous determination of relative angles and anisotropic resistivity using multicomponent induction logging data," *Transactions of 42nd Annual Logging Symposium: Society of Professional Well Logging Analysts*, Houston, Texas, 2001.
27. Zhang, Z. and A. Mezzatesta, "2D anisotropic inversion of multicomponent induction logging data," *Society of Exploration Geophysicists International Exposition and 71st Annual Meeting*, San Antonio, Texas, 2001.
28. Zhang, Z., L. Yu, B. Kriegshäuser, and L. Tabarovsky, "Determination of relative angles and anisotropic resistivity using multicomponent induction logging data," *Geophysics*, Vol. 69, 898–908, 2004.